Investigation of Effect of Flexural and Torsional Moment Values on Optimum RC Beam Design

YASİN DUYSAK, SİNAN MELİH NİGDELİ, GEBRAİL BEKDAŞ
Department of Civil Engineering,
Istanbul University-Cerrahpaşa,
34320 Istanbul,
TURKEY

Abstract: - In reinforced concrete structural design, the sizing and reinforcement of structural elements, as well as the cost-effective fabrication of structural elements and the system, are essential considerations for structural engineers. Today, optimization methods are applied to ensure that structural elements can resist the design loads imposed on them and are sized and reinforced cost-effectively. In this study, in addition to the previous research on the optimum design of the beam section, four different bending moments are considered, and the effects of bending moments and torsional moments are investigated for the optimal cost-effective sizing and reinforcement of reinforced concrete beams. JAYA algorithm is used for beam section design and cost optimization. In this study, four different bending moments and six different torsional moments are applied to the beam section, and a shear force of 150 kN is applied to all beam sections. A total of 48 different beam analyses are performed for two different concrete classes using the MATLAB program. The design constraints and design rules of the widely used ACI 318 code (Building code requirements for structural concrete) are taken into account for beam design. The study clearly shows that an increase in torsional moment leads to an increase in the area of web reinforcement and a decrease in stirrup spacing, while an increase in bending moment leads to an increase in flexural reinforcement. The algorithm can effectively design the beam width and height to enable the beam to efficiently resist the applied moments. It is observed that the JAYA algorithm is effective for optimal beam design under different loads and proves its accuracy in previous studies.

Key-Words: - RC Beams, Beam Section, Section Optimization, Bending Moment, Torsional Moment, Jaya Algorithm.

Received: April 29, 2024. Revised: November 11, 2024. Accepted: December 5, 2024. Published: December 31, 2024.

1 Introduction

In designing reinforced concrete structures, it's essential that structural elements can safely support the loads placed on them. However, today, focusing solely on structural safety is no longer sufficient. Structural engineers must aim for an optimal design that balances structural safety, aesthetics, and cost. Designing reinforced concrete structures is complex and challenging due to concrete's inhomogeneity and isotropy. In traditional methods, the structural engineer determines certain cross-sectional dimensions based on experience and the loads on the element, then reinforces it accordingly. While this approach may allow the element to carry the required loads, it doesn't ensure that the solution is optimal. Achieving a truly cost-effective and optimal design with the traditional method requires repeatedly solving the structural system and selecting the best solution, but this process is both time-consuming and costly. Optimization algorithms have now been developed to find optimal solutions for complex engineering problems. In structural engineering, metaheuristic algorithms are frequently applied, as they combine various search techniques to efficiently reach the best solution while avoiding entrapment in local optima.

In civil engineering, various structural systems and elements have been optimized using different metaheuristic algorithms. One widely applied algorithm in structural engineering is the nature-inspired flower pollination algorithm, [1]. This algorithm has been used in several studies: for cost optimization of reinforced concrete retaining walls using size and reinforcement variables by [2] for weight optimization of L-type reinforced concrete retaining walls by [3] for designing minimum cross-sections of weight retaining walls and comparing them with other algorithms by [4] and for design and cost optimization of two distinct reinforced concrete frame systems by [5].

Inspired by the hunting abilities of bats, the bat algorithm (BA), developed by [6] has been applied in structural engineering by [7] for cost optimization of reinforced concrete columns with varying lengths. Similarly, the harmony search algorithm (HS), inspired by musicians' search for the best melody [8], is also widely used in structural engineering. While HS has been applied to optimization problems in civil engineering, [9] also used it for the optimal design of retaining walls. Additionally, [10] utilized a hybrid approach combining HS with other algorithms to design and optimize reinforced concrete retaining walls.

The genetic algorithm (GA), a well-established method inspired by evolutionary theory [11], is widely applied in civil engineering. [12] applied GA for cost optimization of piled retaining systems, [13] used it for the design and cost optimization of cantilever retaining walls, [14] applied it in the design and cost optimization of concrete-filled composite pipe columns, [15] used it for cost optimization of simply supported and continuous beams, [16] employed it for cost optimization of prestressed reinforced concrete beams, and [17] utilized it for the design of two-dimensional reinforced concrete frame systems, achieving successful outcomes in each case.

Another widely used algorithm in structural engineering is the JAYA algorithm, [18]. The JAYA algorithm is a single-phase algorithm, making it simpler to use than many other metaheuristic approaches. [19] applied it in the optimal cost design of retaining walls and compared it with other metaheuristic algorithms. [20] the effect of the torsional moment on the design of reinforced concrete beam sections, considering ten different beam sections and five different torsional moments, is investigated using the JAYA algorithm. [21] used an improved JAYA-based optimization method to analyze the displacement of 2D and 3D trusses under static loads. [22] applied the JAYA algorithm for the design and cost optimization of steel grid foundation structures and found it effective. Finally, [23] applied the JAYA algorithm to identify damaged areas in structures and to assess the extent of these damages.

In this study, the JAYA algorithm is employed to achieve optimal beam design. The effects of bending and torsional moments on the design and cost of rectangular reinforced concrete beams were examined. To investigate these effects, a constant shear force of 100 kN was applied across all specimens, with four different bending moments and six different torsional moments used. Each design was further analyzed for two concrete classes, C30 and C35, resulting in a total of 48 distinct beam section designs. The design of the reinforced concrete beam was based on ACI 318 (Building Code Requirements for Structural Concrete) [24], with the necessary codes implemented in MATLAB.

2 Methodology

The JAYA algorithm is a population-based optimization method that operates in a single step, making it simpler to use compared to two-step algorithms, which are commonly preferred in fields like civil engineering. Algorithms such as the teaching-learning-based optimization algorithm, flower pollination algorithm, harmony search algorithm, genetic algorithm, and differential evolution algorithm typically involve two distinct phases. By eliminating these multi-phase processes, the JAYA algorithm offers a streamlined, single-phase approach.

The JAYA algorithm begins with randomly assigned design variables and aims to converge on the best solution while moving away from the worst solutions. Initially, the best and worst solutions in the population are identified, and each new solution is updated to lie between these values. The updated solution is then evaluated against specific design constraints and, if it meets these criteria, may be selected as the best solution. This process continues until a predetermined number of iterations or a desired fitness value is reached. The single-step equation of the algorithm is presented below in Equation 1.

$$x_i^{j,t+1} = x_i^{j,t} + r_1(x_i^{*} - |x_i^{j,t}|) - r_2(x_i^{w} - |x_i^{j,t}|) \quad i=1, 2, ..., n ; \; j=1, 2, ..., p ; \; t=1, 2, ..., t_{max} \qquad (1)$$

In Equation 1, (x_i^*) represents the best available solution or the optimal state, while (x_i^w) denotes the worst available solution or the lowest-performing state. In the formula, r_1 and r_2 are random real numbers between 0 and 1, which add flexibility to the solution search process. The term $r_1(x_i^*) - |x_i^{j,t}|)$ drives the solution toward the best state, encouraging convergence toward an optimal result. This allows the solution to gradually approach a better state. Conversely, the term $r_2(x_i^w - |x_i^{j,t}|)$ helps the solution move away from the worst state, thus avoiding poor solutions. By randomizing r_1 and r_2, the algorithm explores a broader design space, enabling it to investigate different areas of the solution space rather than being confined to a specific region. Additionally, the absolute value $|x_i^{j,t}|$ enhances the algorithm's search capability by providing more flexibility. This approach allows the JAYA algorithm to improve outcomes by iteratively comparing available solutions. The process continues until a specified stopping criterion is met, such as reaching a target result or completing a certain number of iterations. Figure 1 illustrates the flow diagram of the JAYA algorithm throughout the solution process.

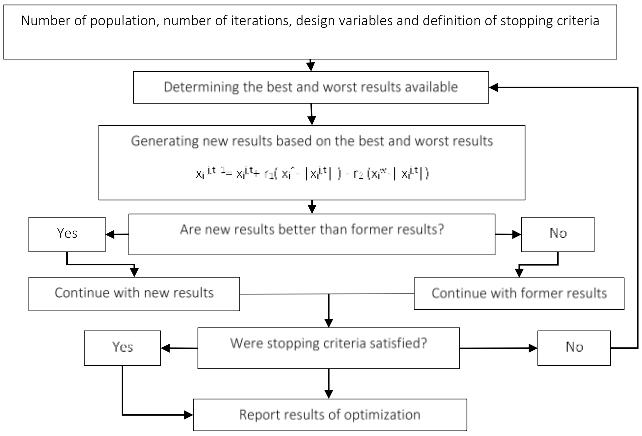

Fig. 1: Flow chart of the optimization method

One of the first and most critical steps in engineering optimization algorithms is defining the problem clearly. During this process, it's essential to identify the problem data, select the variables for the design, establish design constraints, and set the necessary algorithm parameters. In this study, design variables such as the width and height of the beam section, the area of longitudinal reinforcement, the area of shear reinforcement, and the spacing of shear reinforcement were chosen to analyze the effects of torsional and bending moments on beam design. These variables represent fundamental section components that require careful selection in all reinforced concrete designs. Table 1 provides an overview of all design constants and variables used in this study.

Table 1. Design variables and design constants

Explanation	Symbol	Unite	Values
Beam width	h	mm	250-400
Beam depth	b	mm	350-600
Compressive strength of concrete	fck	MPa	30-35
Yield strength of steel	fyk	MPa	420
Modulus of elasticity	E	MPa	27800
The specific density of concrete	γc	t/m3	2.5
The specific density of steel	γs	t/m3	7.86
Concrete cover	d′	mm	40
Stirrup	Ø	mm	8-14
m^3 Cost of concrete (C30)	₺	TL	2800
m^3 Cost of concrete (C35)	₺	TL	3000
Cost of steel	₺	t	27000

The ACI-318, [24], standard is widely adopted in international projects for designing reinforced concrete structures. Since many countries have directly implemented ACI-318, it has become a key guideline in reinforced concrete design. In this study, ACI-318 (Building Code Requirements for Structural Concrete and Commentary) was referenced to define the design constraints and construction rules. For reinforced concrete beams, issues such as durability, safety, and structural integrity are addressed according to ACI-318. This code serves as a trusted reference in projects as it encompasses standards on various aspects, from the dimensioning of reinforced concrete elements to material specifications. Figure 2 illustrates the designed beam section, showing all relevant section shapes and reinforcement types considered in the design process.

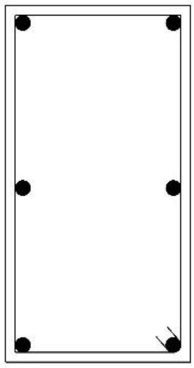

Fig. 2: Details of beam cross-section and reinforcement

As shown in Figure 3, a compression zone forms above the neutral axis in the reinforced concrete element, with the force in this region referred to as Fc, while a tensile zone appears below the neutral axis, where the force is denoted as Fs. When load is applied to the reinforced concrete beam, the concrete in the upper zone resists the compressive force, while the reinforcement in the lower zone resists the tensile force. These forces in the compression and tensile zones work together to maintain equilibrium in the reinforced concrete element, allowing it to support the applied loads.

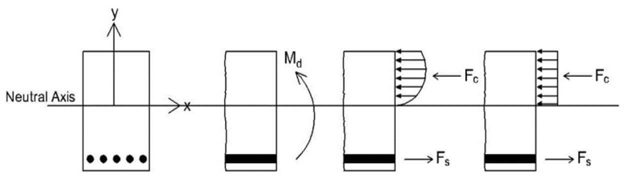

Fig. 3: Actual load distribution and equivalent load distribution in the compression zone

$$F_c = \alpha f'_c ba \quad (2)$$

In Equation 2, the concrete compressive strength is multiplied by the coefficient α (0.85). The parameter a, as shown in Equation 2, represents the depth of the equivalent compression block.

$$a = \beta 1c \quad (3)$$

In Equation 3, c represents the depth of the neutral axis within the compression zone. According to the ACI-318 standard, β_1 defines the equivalent rectangular compression block, and this expression is provided in Equation 4.

$$\beta_1 = 0.85 \qquad 17\ MPa < f'c < 28\ MPa$$
$$\beta_1 = 0.85 - 0.0071428(f'c - 28) \qquad f'c > 28\ MPa \quad (4)$$

The reinforcement tensile force occurring in the tension zone is shown in Equation 5.

$$F_s = A_s f_y \quad (5)$$

In Equation 5, A_s represents the area of tensile reinforcement used in the concrete. When the unit strain of concrete (ε_c) reaches its ultimate strain limit of 0.003, the unit strain of the tensile reinforcement (ε_s) simultaneously reaches the yield strain (ε_{sy}). This condition is referred to as equilibrium fracture. According to the ACI-318 standard, sub-equilibrium fracture must also be considered in beam design. Calculations for sub-equilibrium fracture are based on the balanced reinforcement ratio.

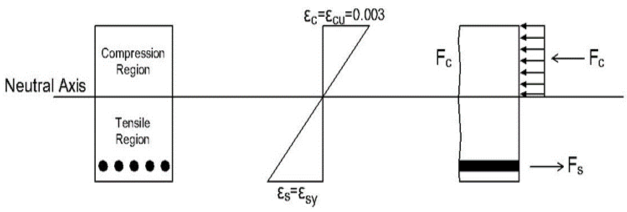

Fig. 4: Internal forced forming in the beam cross-section

Based on the deformation state and internal forces illustrated in Figure 4, the balanced reinforcement ratio ρ_b, which defines the balanced condition, can be determined using Equation 6 when the material properties are known.

$$\rho_b = 0.85\beta_1 \frac{f'c}{f_y}\left(\frac{600}{600+f_y}\right) \quad (6)$$

According to ACI-318, to ensure ductile behavior in beams, the maximum reinforcement ratio should not exceed $\rho_{max}=0.75\rho_b$, and it should not be less than $\rho_{max}=0.025\rho_b$. These limits on the reinforcement ratio are established to achieve ductile beam sections.

According to ACI-318 standard, the minimum longitudinal reinforcement ratio for beams is calculated using Equation 7 and Equation 8.

$$A_{s,min} \geq \frac{\sqrt{f'c}}{4f_y} bd \quad (7)$$

$$A_{s,min} \geq \frac{1.4}{f_y} bd \quad (8)$$

If the calculated reinforcement ratios are lower than the minimum ratios specified in Equations 7 and 8, the minimum longitudinal reinforcement ratio is applied. If the longitudinal reinforcement ratio exceeds the maximum allowable reinforcement ratio, the dimensions of the section are adjusted, and the calculations are performed again. Once the required longitudinal reinforcement for the beam is determined, the design of the stirrups can begin. Rules and limitations set by the regulation on the design of the stirrup;

Maximum shear strength provided by concrete:

$$V_c = 0.17\sqrt{f'_c}bd \quad (9)$$

Maximum shear strength provided by reinforcement:

$$V_s = 0.67\sqrt{f'_c}bd \quad (10)$$

Minimum stirrup area:

$$A_{v,min} = 0.35\frac{b_w s}{f_{yt}} \quad (11)$$

In Equation 11, s represents the distance between stirrups. The distance between shear reinforcements must satisfy the limits in Equation 12, [24].

$$s \leq \begin{cases} d/4 \\ 8\phi_{min} \\ 150\ mm \end{cases} \quad (12)$$

In a structural system, when the torsional moment is not necessary to maintain equilibrium, it is referred to as compliance torsion. Compliance torsion is typically observed in hyperstatic systems. The torsional moment generates shear stresses in the structural elements. To address these stresses, shear reinforcements must be added to the elements, or the shear reinforcement ratio should be increased. According to the ACI-318 standard, when both shear force and torsional moment act on the beam section simultaneously, the rules and limitations set forth by the regulation are given in the following equations.

The limitations required to control the diagonal cracks in the reinforced concrete element due to torsional moment are provided in Equation 13 and Equation 14.

$$\frac{T}{s}+\frac{V}{b_w d}\leq 0.22\, f_{cd} \quad (13)$$

$$\sqrt{\left(\frac{V}{b_w d}\right)^2+\left(\frac{Tp_h}{1.7A_{oh}^2}\right)^2}\leq Ø\left(\frac{V_c}{b_w d}+0.66\sqrt{f'_c}\right) \quad (14)$$

In Equation 14, T represents the torsional moment, p_h is the circumference of the area between the corner reinforcements, A_{oh} is the area between the corner reinforcements, V_c is the shear force, and Ø is the reduction coefficient.

Calculation of the torsional stirrup:

$$A_t=\frac{T\, s}{2ØA_o f_{yt} cot\theta} \quad (15)$$

Shear reinforcement calculation:

$$A_v=\frac{V\, s}{f_{yt} d} \quad (16)$$

The value calculated for torsional stirrup in Equation 15 corresponds to one leg of the stirrup, while the value calculated for shear reinforcement in Equation 16 is for two legs of the stirrup. The total stirrup area for members subjected to both torsional moment and shear force is provided in Equation 17.

$$A_v+t=A_v+2A_t \quad (17)$$

For elements subjected to both torsional moment and shear force, the distance between stirrups is limited by the restrictions provided in Equation 18.

$$s\leq\begin{cases} d/2 \\ ue/8 \\ 300\ mm \end{cases} \quad (18)$$

The total area of the stirrups in members subjected to both torsional moment and shear force is given in Equation 19.

$$A_v+2A_t=0.062\sqrt{f'_c}\,\frac{b_w s}{f_{yt}}\geq 0.35\,\frac{b_w s}{f_{yt}} \quad (19)$$

The minimum web reinforcement area required for beams subjected to torsional moments is provided in Equation 20.

$$A_l=\frac{A_t}{s}p_h\frac{f_{yt}}{f_y}cot^2\theta \quad (20)$$

3 Numerical Example

In this study, 48 different beams were analyzed to investigate the effect of the torsional moment and bending moment on the optimum cost design of the beam section. After dimensioning and equipping the beam section, the cost of a 1-meter beam was calculated, and the results were compared. The loads acting on the beam section are illustrated in Figure 5.

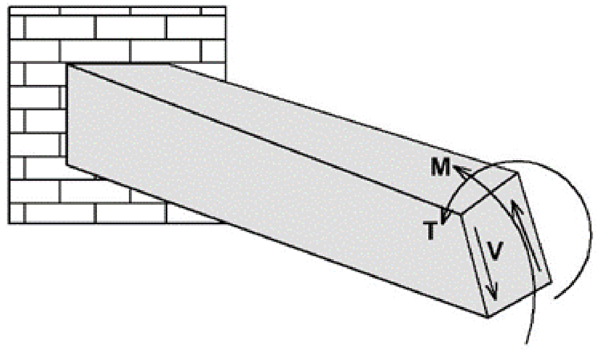

Fig. 5: Loads acting on the beam section

The shear force was assumed to be 100 kN for all beam specimens. A total of 4 different bending moments (50 kNm, 100 kNm, 150 kNm, and 200 kNm) and 6 different torsional moments (0 kNm, 10 kNm, 20 kNm, 30 kNm, 40 kNm, and 50 kNm) were considered in the study. Each beam specimen was designed and compared separately for C30 and C35 concrete classes, resulting in a total of 48 different beams being analyzed. In the nomenclature of the beam specimens, "B" refers to the beam, the first numerical value indicates the bending moment acting on the beam, the second numerical value indicates the torsional moment acting on the beam section, and "L" denotes concrete with a compressive strength of 30 MPa, while "H" indicates concrete with a compressive strength of 35 MPa.

Table 2, Table 3, Table 4 and Table 5 present all the data obtained from the analysis. No web reinforcement was used for the specimens with a zero (0) torsional moment.

Tablo 2. Beam Design Results Under a 50 kNm Bending Moment and 100 kN Shear Force

Sample Number	Concrete Class	Torsional Moment (kNm)	Flexural Reinforcement (mm2)	Web Reinforcement (mm2)	Stirrup Reinforcement (d/s)	Section (b_w/h) mm	Cost ₺
B50-0/L	C30	0 kNm	401.12	0	Ø8/110	25/35	365.73
B50-0/H	C35		398.49	0	Ø8/110	25/35	382.67
B50-10/L	C30	10 kNm	401.12	358.02	Ø8/77.7	25/35	456.53
B50-10/H	C35		398.49	358.02	Ø8/80.4	25/35	471.78
B50-20/L	C30	20 kNm	341.35	672.82	Ø8/58.7	25/40	574.26
B50-20/H	C35		339.74	672.82	Ø8/60.3	25/40	591.91
B50-30/L	C30	30 kNm	352.11	859.43	Ø8/55.2	30/40	701.95
B50-30/H	C35		380.32	859.43	Ø8/56.8	30/40	728.82
B50-40/L	C30	40 kNm	401.01	1082.82	Ø8/51.4	30/45	828.16
B50-40/H	C35		394.13	1106.61	Ø8/50.0	35/35	810.41
B50-50/L	C30	50 kNm	449.91	1293.44	Ø8/50.0	30/50	947.68
B50-50/H	C35		443.71	1275.20	Ø8/50.0	35/40	932.25

Tablo 3. Beam Design Results Under a 100 kNm Bending Moment and 100 kN Shear Force

Sample Number	Concrete Class	Torsional Moment (kNm)	Flexural Reinforcement (mm2)	Web Reinforcement (mm2)	Stirrup Reinforcement (d/s)	Section (b_w/h) mm	Cost ₺
B100-0/L	C30	0 kNm	843.69	0	Ø8/110.0	25/35	459.65
B100-0/H	C35		830.94	0	Ø8/110.0	25/35	474.45
B100-10/L	C30	10 kNm	610.68	320.64	Ø8/121.9	25/45	556.67
B100-10/H	C35		699.78	336.41	Ø8/102.4	25/40	565.22
B100-20/L	C30	20 kNm	610.68	641.27	Ø8/70.9	25/45	656.42
B100-20/H	C35		606.01	641.27	Ø8/73.1	25/45	675.61
B100-30/L	C30	30 kNm	538.35	925.86	Ø8/58.6	25/50	764.74
B100-30/H	C35		535.18	925.86	Ø8/60.1	25/50	786.43
B100-40/L	C30	40 kNm	605.25	1082.82	Ø8/51.4	30/45	871.50
B100-40/H	C35		479.59	1196.64	Ø8/52.8	25/55	897.45
B100-50/L	C30	50 kNm	534.66	1293.44	Ø8/50.0	30/50	965.66
B100-50/H	C35		532.08	1293.44	Ø8/50.0	30/50	994.82

Tablo 4. Beam Design Results Under a 150 kNm Bending Moment and 100 kN Shear Force

Sample Number	Concrete Class	Torsional Moment (kNm)	Flexural Reinforcement (mm2)	Web Reinforcement (mm2)	Stirrup Reinforcement (d/s)	Section (b_w/h) mm	Cost ₺
B150-0/L	C30	0 kNm	1103.48	0	Ø8/122.5	25/40	552.07
B150-0/H	C35		998.27	0	Ø8/122.5	25/40	567.00
B150-10/L	C30	10 kNm	825.16	308.62	Ø8/147.5	25/50	631.92
B150-10/H	C35		817.41	308.62	Ø8/147.5	25/50	655.27
B150-20/L	C30	20 kNm	735.19	598.32	Ø8/99.1	25/55	736.77
B150-20/H	C35		817.41	617.24	Ø8/87.5	25/50	749.15
B150-30/L	C30	30 kNm	735.19	897.48	Ø8/67.9	25/55	831.96
B150-30/H	C35		729.76	897.48	Ø8/69.9	25/55	855.35
B150-40/L	C30	40 kNm	663.66	1166.07	Ø8/58.7	25/60	936.88
B150-40/H	C35		729.76	1196.67	Ø8/52.8	25/55	950.55
B150-50/L	C30	50 kNm	816.15	1293.44	Ø8/50.0	30/50	1025.4
B150-50/H	C35		809.95	1293.44	Ø8/50.0	30/50	1054.1

Tablo 5. Beam Design Results Under a 200 kNm Bending Moment and 100 kN Shear Force

Sample Number	Concrete Class	Torsional Moment (kNm)	Flexural Reinforcement (mm2)	Web Reinforcement (mm2)	Stirrup Reinforcement (d/s)	Section (b_w/h) mm	Cost ₺
B200-0/L	C30	0 kNm	1125.98	0	Ø8/147.5	25/50	630.26
B200-0/H	C35		1073.49	0	Ø8/147.5	25/50	645.42
B200-10/L	C30	10 kNm	998.05	299.16	Ø8/160.0	25/55	702.91
B200-10/H	C35		987.72	299.16	Ø8/160.0	25/55	728.21
B200-20/L	C30	20 kNm	897.75	583.04	Ø8/115.8	25/60	799.42
B200-20/H	C35		987.72	598.32	Ø8/103.6	25/55	814.90
B200-30/L	C30	30 kNm	897.75	874.56	Ø8/77.9	25/60	892.99
B200-30/H	C35		890.31	874.56	Ø8/79.3	25/60	919.65
B200-40/L	C30	40 kNm	897.75	1166.07	Ø8/58.7	25/60	986.56
B200-40/H	C35		890.31	1166.07	Ø8/59.5	25/60	1013.2
B200-50/L	C30	50 kNm	986.04	1246.14	Ø8/55.7	30/55	1094.2
B200-50/H	C35		977.82	1246.14	Ø8/55.7	30/55	1125.5

As seen in Figure 6, in the absence of a torsional moment, the cost of the beam specimens increases with the increase in the bending moment. In the beam specimens where the bending moment remains constant, an increase in the torsional moment leads to a rise in the cost of the beam. Additionally, it is observed that an increase in concrete quality slightly raises the beam's cost due to the higher cost of concrete.

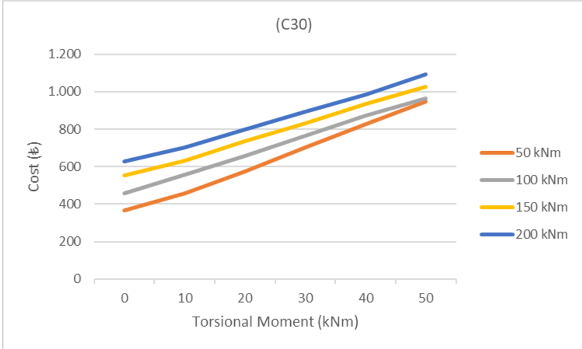

a)C30

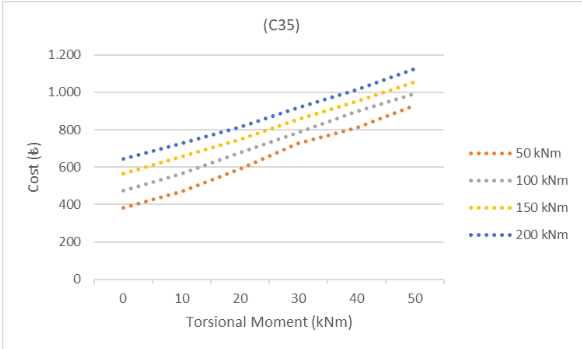

b)C35

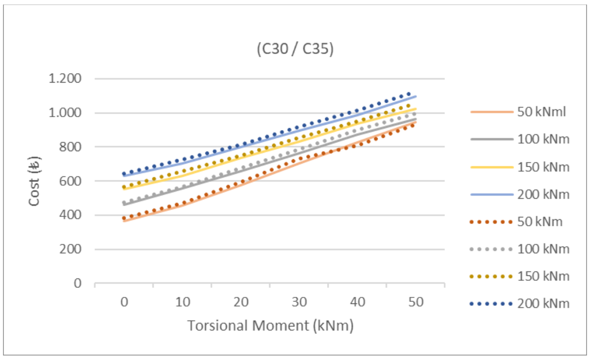

c)C30 - C35

Fig. 6: Effect of the torsional moment on beam cost

As seen in Figure 7, in the specimens where all cross-sectional effects are the same but the torsional moment differs, an increase in the torsional moment raises the cost of the beam. In specimens where the other forces, except the bending moment, remained constant, the cost of the beam increased with the rise in the bending moment. When comparing Figure 6 and Figure 7, it is evident that the effect of the bending moment on the cost is less significant than the effect of the torsional moment.

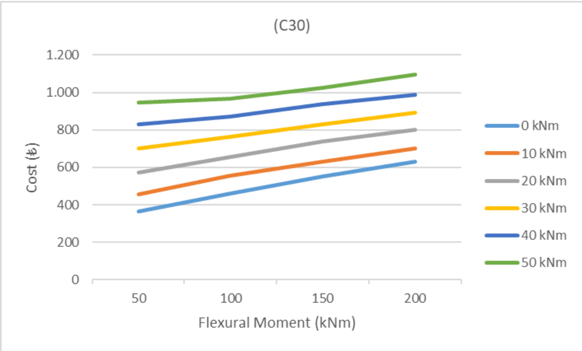

a)C30

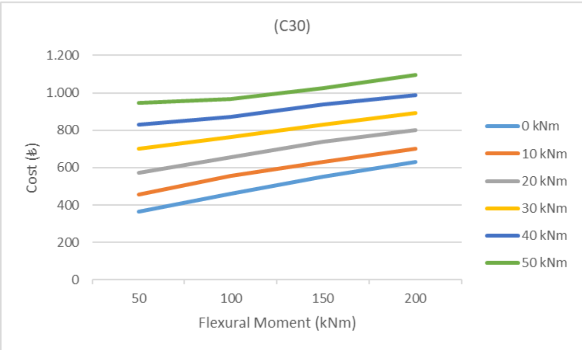

b)C35

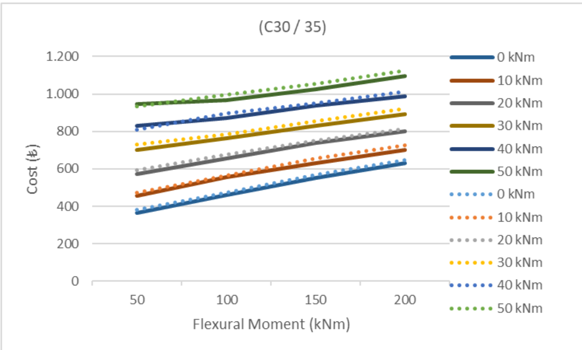

c)C30 – C35

Fig. 7: Effect of bending moment on cost

As seen in Figure 8, the area of the beam cross-section increases with the increase in torsional moment. To counteract the torsional moment, the algorithm not only increases the cross-sectional area but also enhances the bearing capacity of the cross-section by adjusting the reinforcement areas or stirrup spacing in some cases.

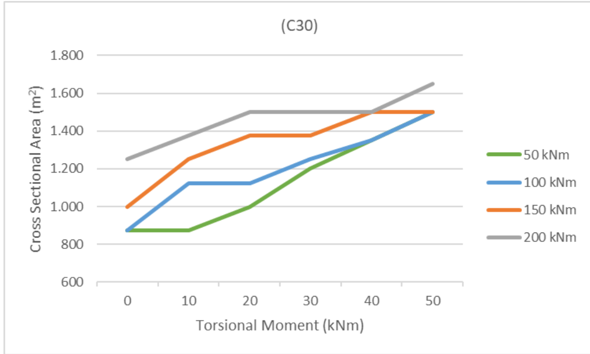

a)C30

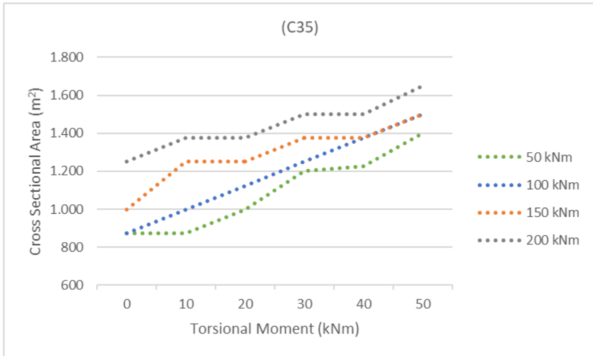

b)C35

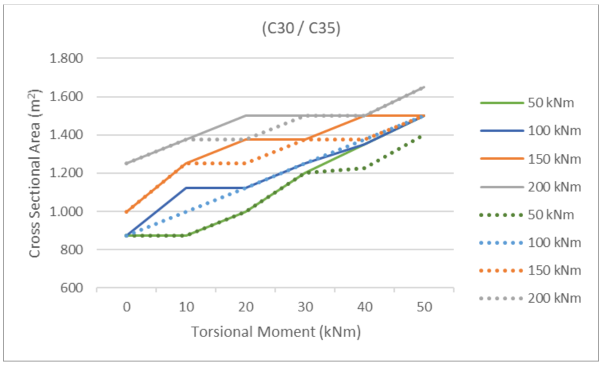

c)C30 – C35

Fig. 8: Effect of the torsional moment on the cross-sectional area

As seen in Figure 9, the area of the beam section increases with the increase in bending moment. To resist the bending moment, the algorithm not only increases the cross-sectional area but, in some cases, enhances the bearing capacity of the cross-section by adjusting the reinforcement areas or stirrup spacing. When comparing Figure 8 and Figure 9, it is evident that the effect of the bending moment on the increase in section area is less significant than the effect of the torsional moment.

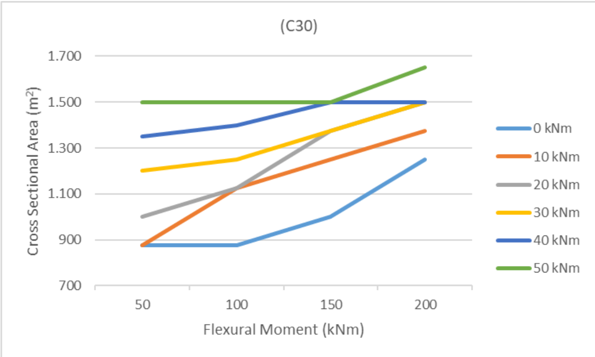

a)C30

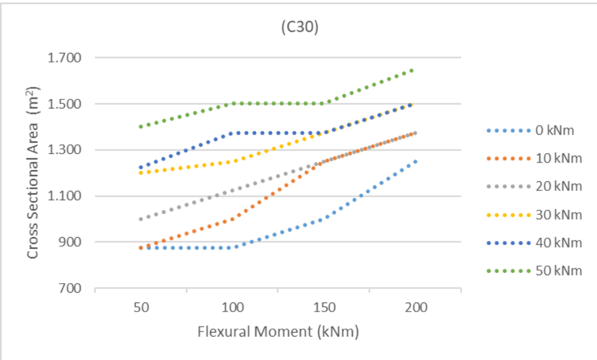

b)C35

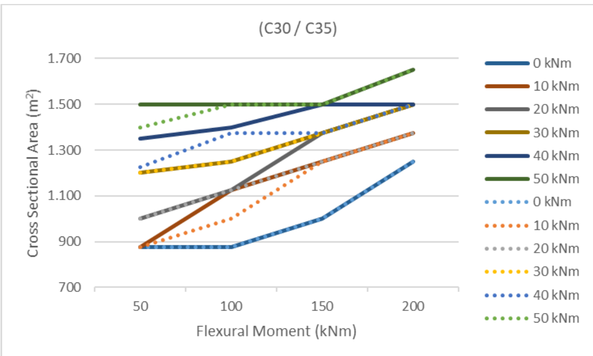

c)C30 – C35

Fig. 9: Effect of bending moment on cross-sectional area

The effect of the increase in bending moment on the increase in flexural reinforcement is shown in Figure 10.

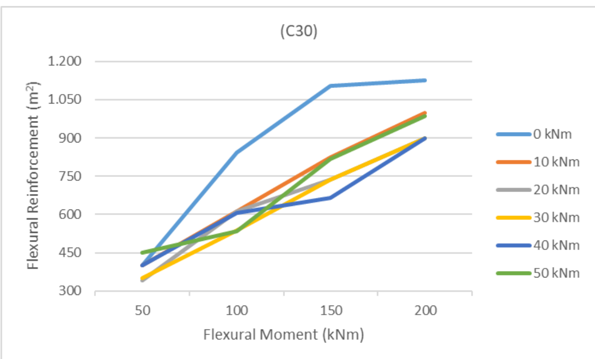

a)C30

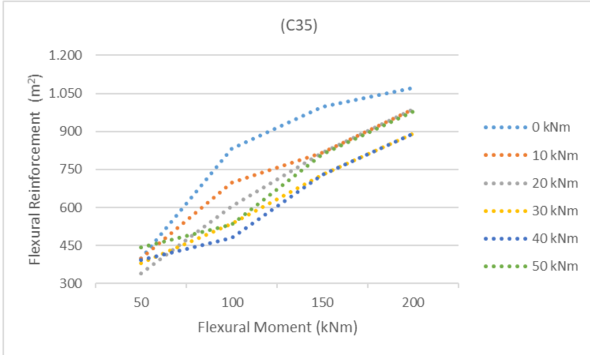

b)C35

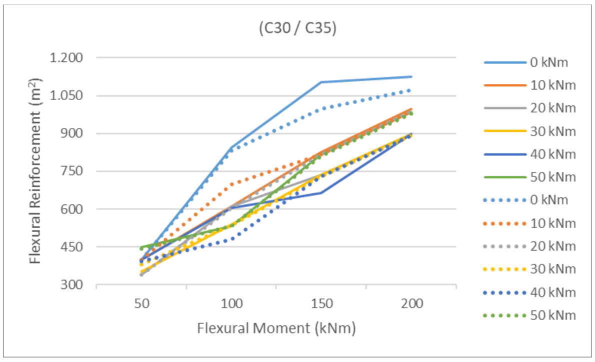

c)C30 – C35

Fig. 10: Effect of bending moment on flexural reinforcement

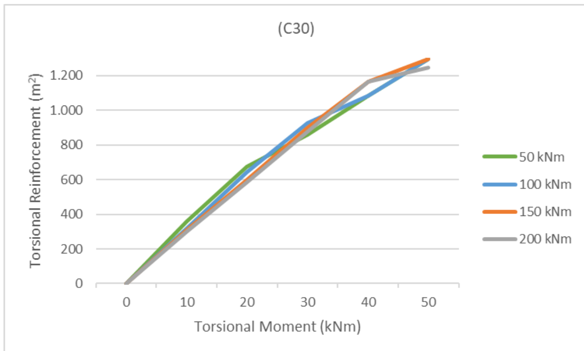

a)C30

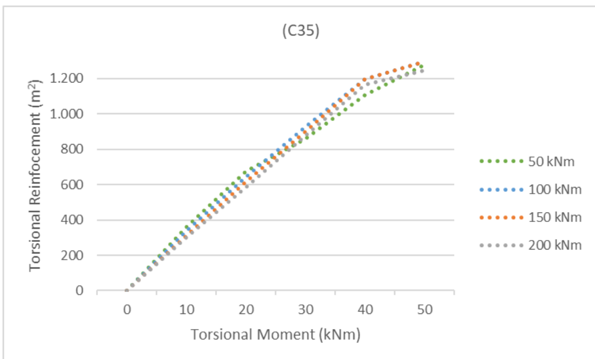

b)C35

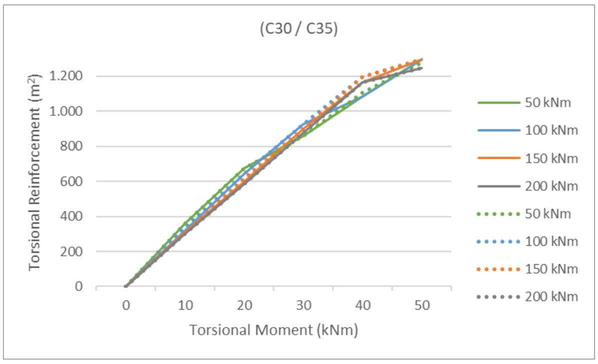

c)C30 – C35

Fig. 11: Effect of the torsional moment on web reinforcement

The effect of the increase in torsional moment on the increase in torsional reinforcement is shown in Figure 11.

4 Conclusion

In this paper, the impact of bending and torsional moments on the cost of beam sections is analyzed using the JAYA algorithm. The analysis of 48 different beams shows that as the torsional and bending moments increase, all factors contributing to the cost also rise.

- The increase in the bending moment acting on the beam section leads the algorithm to first prioritize increasing the beam height (h). This approach is adopted because concrete is considered more effective than reinforcement in resisting bending moments.
- With the effect of the torsional moment acting on the beam section, a significant increase in the web reinforcement ratio, a decrease in stirrup spacing, and an increase in the section width (b) were observed.
- With the increase in concrete quality, a slight decrease in flexural reinforcement and an increase in stirrup spacing are observed. However, the higher cost of C35 concrete compared to C30 concrete prevents a reduction in overall costs.
- The increase in torsional moment has a more significant effect on both the beam area and the overall beam cost compared to the increase in bending moment.
- The presence of web reinforcement reduces the required area of flexural reinforcement.
- The JAYA algorithm was found to be effective in beam design and optimization. In this study, considered a continuation of the previous research, the accuracy of the JAYA algorithm was further confirmed through the analysis results.

Declaration of Generative AI and AI-assisted Technologies in the Writing Process

The authors wrote, reviewed and edited the content as needed and they have not utilised artificial intelligence (AI) tools. The authors take full responsibility for the content of the publication

References:

[1] Yang, X.S., Flower Pollination Algorithm for Global Optimization, *International Conference on Unconventional Computing and Natural Computation*, Springer, Berlin, Heidelberg, 2012, pp. 240-249. doi: 10.1007/978-3-642-32894-7_27

[2] Yılmaz, B., Bekdaş, G., Nigdeli, S. M., Betonarme İstinat Duvarlarının Çiçeklerin Tozlaşma Algoritması ile Optimizasyonu, *XIX. Ulusal Mekanik Kongresi*, Trabzon, 2015 pp. 1070-1075.

[3] Kayabekir, A. C., Yücel, M., Bekdaş, G., Nigdeli, S. M., Comparative Study of Optimum Cost Design of Reinforced Concrete Retaining Wall via Metaheuristics, *Challenge Journal of Concrete Research Letters*, Vol.11, No.3, 2020, pp. 75-81. doi: 10.20528/cjcrl.2020.03.004

[4] Lyu, P., Luo, Q., Wang, T., Connolly, D.P., Railway Gravity Retaining Wall Design Using the Flower Pollination Algorithm, *Transportation Geotechnics*, Vol. 42, No.101065, 2023, pp. 1-15. doi: 10.1016/j.trgeo.2023.101065

[5] Panagiotis E. M., Optimum Design of 3D Reinforced Concrete Building Frames with the Flower Pollination Algorithm. *Journal of Building Engineering*, Vol. 44, No.102935, 2021, pp. 1-13. doi: 10.1016/j.jobe.2021.102935

[6] Yang, X.S., A New Metaheuristic Bat-inspired Algorithm, *Nature Inspired Cooperative Strategies for Optimization (NICSO 2010)*, Heidelberg, 2010, pp. 65-74. doi: 10.1007/978-3-642-12538-6_6

[7] Vu-Huu, T., Pham-Van, S., Pham, Q., Cuong-Le, T., An Improved Bat Algorithms for Optimization Design of Truss Structures, *Structures*, Vol.47, 2023, pp. 2240-2258. doi: 10.1016/j.istruc.2022.12.033

[8] Geem, Z. W., Kim, J. H., Loganathan, G. V., A New Heuristic Optimization Algorithm:

Harmony search, *Simulation*, Vol.76, No.2, 2001, pp. 60–68. doi: 10.1177/003754970107600201

[9] Kaveh, A., Abadi, S. M., Harmony Search Based Algorithms for the Optimum Cost Cesign of Reinforced Concrete Cantilever Retaining Walls, *International Journal of Civil Engineering*, Vol.9, No.1, 2010, pp. 1-8, [Online]. http://ijce.iust.ac.ir/article-1-292-en.html (Accessed Date: October 15, 2024).

[10] Sheikholeslami, R., Khalili, B. G., Sadollah, A., Kim, J. H., Optimization of Reinforced Concrete Retaining Walls via Hybrid Firefly Algorithm with Upper Bound Strategy, *KSCE Journal of Civil Engineering*, Vol.20, No.6, 2016, pp. 2428-2438. doi: 10.1007/s12205-015-1163-9.

[11] Goldberg, D. E., Samtani, M. P., Engineering Optimization via Genetic Algorithm, *Proceedings of Ninth Conference on Electronic Computation*, ASCE, New York, 1986, pp. 471-482, [Online]. https://api.semanticscholar.org/CorpusID:59505228 (Accessed Date: October 15, 2024).

[12] Taiyari, F., Kharghani, M., Hajihassani, M., Optimal Design of Pile Wall Retaining System During Deep Excavation Using Swarm İntelligence Technique, *Structures*, Vol.28, 2020, pp. 1991-1999. doi: 10.1016/j.istruc.2020.10.044.

[13] Pei, Y., Xia, Y., Design of Reinforced Cantilever Retaining Walls using Heuristic Optimization Algorithms, *Procedia Earth and Planetary Science*, Vol.5, 2012, pp. 32-36. doi: 10.1016/j.proeps.2012.01.006.

[14] Guimarães, S. A., Klein, D., Calenzani, A. F. G., Alves, E. C., Optimum Design of Steel Columns Filled with Concrete via Genetic Algorithm: Environmental Impact and Cost Analysis, *International Engineering Journal*, Vol.75, No.2, 2022, pp. 117-128. doi: 10.1590/0370-44672021750034.

[15] Pierott, R., Hammad, A. W. A., Haddad, A., Garcia, S., Falcon, G., A Mathematical Optimisation Model for the Design and Detailing of Reinforced Concrete Beams, *Engineering Structures*, Vol.245, 2021, 112861. doi: 10.1016/j.engstruct.2021.112861.

[16] Alqedra, M., Arafa, M., İsmail, M., Optimum Cost of Prestressed and Reinforced Concrete Beams using Genetic Algorithms, *Journal of Artificial Intelligence*, Vol.4, No.1, 2011, pp. 76-88. doi: 10.3923/jai.2011.76.88.

[17] Shooli, A. R., Vosoughi, A. R., Banan, M. R., A mixed GA-PSO-Based Approach for Performance-Based Design Optimization of 2D Reinforced Concrete Special Moment-Resisting Frames, *Applied Soft Computing Journal*, Vol.85, 2019, 105843. doi: 10.1016/j.asoc.2019.105843.

[18] Rao, R., Jaya: A Simple and new Optimization Algorithm for Solving Constrained and unconstrained Optimization Problems, *International Journal of Industrial Engineering Computations*, Vol.7, No.1, 2016, pp. 19-34. doi: 10.5267/j.ijiec.2015.8.004.

[19] Öztürk, H. T., Dede, T., Türker, E., Optimum Design of Reinforced Concrete Counterfort Retaining Walls Using TLBO, Jaya Algorithm, *Structures*, Vol.25, 2020, pp. 285-296. doi: 10.1016/j.istruc.2020.03.020.

[20] Duysak, Y., Nigdeli, S. M., Bekdaş, G., Optimum Design of Reinforced Concrete Beam Sections with JAYA Algorithm, *Challenge Journal of Concrete Research Letters*, Vol.15, No.4, 2024, pp.134-141. doi: 10.20528/cjcrl.2024.04.003.

[21] Pham, H. A., Nguyen, B. D., Fuzzy Structural Analysis Using Improved Jaya-based Optimization Approach, *Periodica Polytechnica Civil Engineering*, Vol.68, No.1, 2024, pp. 1-7. doi: 10.3311/PPci.22818.

[22] Dede, T., Jaya Algorithm to solve Single Objective Size Optimization Problem for Steel Grillage Structures, *Steel and Composite Structures*, Vol.26, No.2, 2018, pp. 163-170. doi: 10.12989/scs.2018.26.2.163.

[23] Du, D. C., Vinh, H. H., Trung, V. D., Quyen, N. T. H., Trung, N. T., Efficiency of Jaya Algorithm for Solving the Optimization-Based Structural Damage Identification Problem Based on A Hybrid Objective Function, *Engineering Optimization*, Vol.50, No.8, 2018, pp. 1233-1251. doi: 10.1080/0305215X.2017.1367392.

[24] ACI Committee, *Building Code Requirements for Structural Concrete (ACI 318-05) and Commentary*. American Concrete Institute, & International Organization for Standardization, American Concrete Institute, 2008.

Contribution of Individual Authors to the Creation of a Scientific Article (Ghostwriting Policy)

This work is a collaboration between the three authors. The authors equally contributed in the present research, at all stages from the formulation of the problem to the final findings and solution.

Sources of Funding for Research Presented in a Scientific Article or Scientific Article Itself

No funding was received for conducting this study.

Conflict of Interest

The authors have no conflicts of interest to declare.